

Uncovering Latent Connections in Indigenous Heritage: Semantic Pipelines for Cultural Preservation in Brazil

Luis Vitor Zerkowski¹, Nina S. T. Hirata²

¹University of Amsterdam

²University of São Paulo

luisvz@gmail.com, nina@ime.usp.br

Abstract

Indigenous communities face ongoing challenges in preserving their cultural heritage, particularly in the face of systemic marginalization and urban development. In Brazil, the *Museu Nacional dos Povos Indígenas* through the *Tainacan* platform hosts the country's largest online collection of Indigenous objects and iconographies, providing a critical resource for cultural engagement. Using publicly available data from this repository, we present a data-driven initiative that applies artificial intelligence to enhance accessibility, interpretation, and exploration. We develop two semantic pipelines: a visual pipeline that models image-based similarity and a textual pipeline that captures semantic relationships from item descriptions. These embedding spaces are projected into two dimensions and integrated into an interactive visualization tool we also developed. In addition to similarity-based navigation, users can explore the collection through temporal and geographic lenses, enabling both semantic and contextualized perspectives. The system supports curatorial tasks, aids public engagement, and reveals latent connections within the collection. This work demonstrates how AI can ethically contribute to cultural preservation practices.

Code — https://github.com/Luizerko/indigenous_clusters_and_communities

Data — <https://tainacan.museudoindio.gov.br/>

Introduction

Indigenous peoples in Brazil continue to face cultural erasure, land dispossession, and limited visibility despite constitutional protections and growing public awareness. Preserving Indigenous knowledge - its languages, symbols, and histories - is both an ethical imperative and a technological challenge. Public institutions have begun to digitize important collections to support cultural preservation; among them, the *Museu Nacional dos Povos Indígenas* (mus 2025) through the *Tainacan* platform (tai 2025) hosts Brazil's largest online repository of Indigenous objects and iconographies. While this represents a major step forward, the collection remains difficult to explore due to limited semantic organization and interactivity.

This work proposes a data-driven system that enhances access to this digital collection using artificial intelligence.

Copyright © 2026, Association for the Advancement of Artificial Intelligence (www.aaai.org). All rights reserved.

We present two semantic pipelines: one that models visual similarity using features extracted from item images, and another that captures semantic relationships from textual descriptions. Each pipeline produces an embedding space, projected to two dimensions for interactive visualization. These structured representations are integrated into a developed point-cloud interface that enables users to explore the collection through similarity-based navigation.

In addition to semantic exploration, the tool offers browsing through temporal and geographic lenses, offering more traditional, contextualized views of the data. The system supports both public engagement and curatorial analysis by revealing mislabeled items, surfacing latent connections, and suggesting new interpretive directions. It is fully open-source and designed for transparency and reuse, with code, documentation, and dataset references available at will_be_available_on_camera-ready.

Related Work

Preserving Indigenous heritage is both a cultural and technological challenge, particularly in countries like Brazil with immense Indigenous diversity. Digital technologies have played a growing role in this space, enabling broader accessibility and engagement (Muñoz and Tisi 2020). In education, *Guimarães* (Guimarães 2015) and *Ferreira* (Ferreira 2011) emphasize the need to integrate Indigenous perspectives dynamically rather than as static representations, while others highlight connections to biodiversity and linguistic preservation (Wilder et al. 2016).

Platforms like *Mukurtu CMS* (Center for Digital Scholarship and Curation, Washington State University 2025)¹ and repatriation projects (Rebellato 2025) aim to involve Indigenous communities in curatorial processes. Still, most remain reliant on metadata-driven interfaces, which can limit deeper semantic engagement (Alma'aitah, Talib, and Osman 2020). To address this, researchers have explored semantic modeling and AI-based design to enrich representation fidelity and interactivity.

Recent progress in computer vision and language modeling offers a technical foundation for working with cultural data. Vision models such as U-Net (Ronneberger, Fischer, and Brox 2015) and modern transformers like ViT (Doso-

¹<https://mukurtu.org/>

vitskiy et al. 2021), SAM (Kirillov et al. 2023), and DINOv2 (Oquab et al. 2023) enhance image-based analysis. In the textual domain, models like BERTimbau (Souza, Nogueira, and Lotufo 2020) and Albertina (Rodrigues et al. 2023), often trained with contrastive learning (Gao, Yao, and Chen 2021; Liao 2021), enable nuanced sentence-level embeddings. Cross-modal models such as CLIP (Radford et al. 2021) open up further opportunities for aligning imagery and text.

To make these embeddings interpretable and user-friendly, dimensionality reduction techniques like UMAP (McInnes, Healy, and Melville 2018), t-SNE (van der Maaten and Hinton 2008), and TriMap (Amid and Warmuth 2019) are often used to project embedding spaces into 2D or 3D plots. Tools such as the Embedding Projector² (Smilkov et al. 2016) exemplify how interactive visualizations can enhance exploration. Similarly, interpretability-focused initiatives like the Activation Atlas³ (Carter et al. 2019) offer engaging, exploratory views of complex models and datasets.

Importantly, Indigenous digital protagonism (Hisayasu 2019) stresses the active role of Indigenous communities in shaping how their histories are represented online, reinforcing the need for tools that are not only technically robust, but also culturally inclusive by design.

Contributions

This work offers three main contributions. First, we developed a complete data processing pipeline for the Indigenous collection of the *Museu Nacional dos Povos Indígenas*, including documentation, practical guidelines, and machine-learning-ready datasets with background-removed images and summarized descriptions, all shared with the museum. Second, we introduced a modular dual-pipeline framework for modeling visual and textual similarity, adapted to Brazilian Portuguese and the visual specificity of Indigenous items. The framework supports various architectures and training strategies and is designed for reuse across collections. Lastly, we implemented an interactive semantic visualization tool for exploring the collection through embedding point-clouds, as well as temporal and geographic views. Designed for both public and curatorial use, it is scheduled for deployment on Brazil’s federal government website.

Data Gathering and Processing

The dataset employed in this work was extracted from the public *Tainacan* repository (tai 2025), with a focus on the collection curated by the *Museu Nacional dos Povos Indígenas* (mus 2025). Metadata from 20,965 items was collected via custom Bash and Python scripts, with data usage authorized by the museum. Key attributes include the item’s category (*categoria*), Indigenous community (*povo*), thumbnail image (*thumbnail*), and full-text description (*descricao*).

Following extraction, the dataset underwent preprocessing tailored to visual and textual modeling pipelines.

For images, we applied background removal using the RMBG-2.0 model (Zheng et al. 2024). This step mitigated risks of spurious visual correlations across the 11,274 items (the ones with image data). Text descriptions were lowercased and then, to meet GPU memory constraints (8GB VRAM) and enhance representation learning, we implemented a summarization pipeline targeting a 64-token maximum. This was achieved using the Llama-4-Maverick-17B-128E-Instruct model (Touvron et al. 2023), accessed via the Groq API (gro 2025)⁴. The prompts emphasized semantic retention, prioritizing details and cultural vocabulary.

Building on the summarized corpus, we constructed contrastive learning datasets. For the supervised setup, each anchor was paired with a paraphrased positive, generated via the aforementioned large language model (LLM), and ten negative examples randomly sampled from different *categoria* labels, to ensure semantic dissimilarity.

Now for evaluating both supervised and unsupervised models, we also developed a benchmark called In-Context STS-B. For each item, we used the LLM-generated paraphrase as a positive example, but additionally asked the LLM to select the most semantically distinct description of a chunk as a negative example. Because our chunks were originally designed for description summarization though, they contained sequential data. While this occasionally led to highly similar descriptions grouped and hence some false negatives, the dataset still offered useful insights into contextualized semantic sensitivity.

Constructing Semantic Spaces

With the dataset fully processed, we turn to constructing semantic spaces that reflect the visual and textual similarities among cultural artifacts. Our goal is twofold: to build practical tools that facilitate intuitive exploration of large archival datasets, and to demonstrate how machine learning can augment human curation by revealing latent structures within collections. This section begins with baselines grounded in domain knowledge. These methods do not rely on learning from data but instead leverage metadata and interpretable encodings to establish reference points. While limited in representational capacity, they were thought of to validate the output of more complex models, but also illustrate the limitations of purely categorical representations.

Baselines from Metadata Encodings

Before arriving at the final pipeline, we tested several metadata-based strategies to explore direct semantic relationships within the collection. These included orthonormal projections of categorical attributes, K-Modes clustering (Huang 1998) over multi-hot metadata, and even a triangular layout based solely on *tipo_de_materia_prima*. While each method was analytically interpretable, none yielded sufficiently coherent or generalizable semantic groupings. Dimensionality reduction techniques such as UMAP (McInnes, Healy, and Melville 2018), TriMap (Amid and Warmuth 2019), and t-SNE (van der Maaten

²<https://projector.tensorflow.org/>

³<https://distill.pub/2019/activation-atlas/>

⁴<https://groq.com/>

and Hinton 2008) also produced noisy, meaningless projections. We further explored the use of language family trees as a reference taxonomy but found them too fragmented and inconsistent for computational use.

This reframed the role of our semantic models: rather than validating against fixed baselines, they become tools for surfacing latent patterns and generating curatorial hypotheses. Both visual and textual embeddings support the discovery of connections and inconsistencies not captured by existing metadata. In this way, our platform offers a starting point for deeper curatorial inquiry and interdisciplinary collaboration. Full implementation details and evaluations of the early strategies can be found in the extended version of this work and in the public repository documentation.

Image-Based Semantic Spaces

To understand visual relationships among collection items, we developed a deep learning-based image pipeline. We extracted embeddings from background-removed images using two transformer-based architectures, ViT Base (Dosovitskiy et al. 2021) and DINOv2 Base (Oquab et al. 2023), and projected the resulting representations into 2D for qualitative analysis. Among dimensionality reduction techniques tested, UMAP yielded the clearest manifolds.

Fine-Tuning Strategy: Our initial approach to fine-tuning (a second one will be introduced later for textual embeddings) relied on simple supervised learning using existing attributes in the dataset as targets. While the pretrained visual models already displayed reasonable semantic structure, verified through qualitative inspection, we sought to further refine this structure and inject higher-level semantic alignment. To achieve this, we used supervised training with the `povo` and `categoria` attributes as targets.

We followed standard fine-tuning practices from the ViT literature (Dosovitskiy et al. 2021; Steiner et al. 2022), attaching a single linear classification head on top of the transformer backbone. The same architecture was used for DINOv2 to enable fair comparison. Models were trained until convergence, typically between 10 and 20 epochs, with early stopping applied. While we explored a broad range of hyperparameters, we report only the most representative and effective configurations - those sufficient to illustrate performance trends across different values. Each configuration was trained multiple times to report mean and standard deviation across runs.

Class imbalance was a major challenge, especially for `povo`, which includes 187 classes, many with only a handful of samples. To address this, we implemented a rebalancing strategy combining class filtering, data augmentation, and weighted loss functions, a combination that consistently improved performance across evaluation metrics. We also experimented with layer freezing (starting from the bottom up) to preserve general knowledge in early layers.

We later introduced a multi-head setup to jointly optimize for both `povo` and `categoria`, aiming to explore whether combining distinct semantic signals would enrich the learned representations. For this setup, all training used a rebalanced dataset, focusing solely on `povo`, since attempt-

ing to rebalance both attributes either reintroduced imbalance in the other or failed due to extreme sparsity in the joint distribution. As discussed later, this configuration yielded particularly interesting numerical and qualitative results.

Evaluation: Since the original models lacked classification heads, we couldn’t numerically compare performances with them. For quantitative analysis on the fine-tuned models, however, we measured accuracy, precision, and recall across all trained models. Given the severe class imbalance, particularly for `povo`, we introduced refined metrics - Precision/Recall (Selected) - which evaluate performance only on the subset of classes used in the rebalanced dataset. This allows a fair comparison between models trained with and without rebalancing, as evaluating on unseen classes would be misleading for the rebalanced models.

Finally, we visually examined the embedding spaces produced by each model to assess not only dispersion but also the emergence of coherent clusters aligned with the target attributes. This qualitative inspection served as an additional layer of validation for the models’ representational quality.

ViT-Based Models: Results are summarized in Tables 1, 2 and 3.

Training Data	Frozen (%)	Acc. (%)	Prec. Sel.	Rec. Sel.
Original	0	68.32 ± 1.52	0.58 ± 0.01	0.62 ± 0.01
Rebalanced	0	70.99 ± 0.73	0.71 ± 0.02	0.69 ± 0.02
Rebalanced	80	67.48 ± 1.13	0.64 ± 0.01	0.62 ± 0.01

Table 1: Test set performance of fine-tuned ViT models on the `povo` classification task. Models were (mostly) trained with a learning rate of 2×10^{-5} , a weight decay of 2×10^{-6} , and weighted loss inversely proportional to class frequency.

Training Data	Frozen (%)	Acc. (%)	Prec. Sel.	Rec. Sel.
Original	0	87.60 ± 0.81	0.86 ± 0.02	0.84 ± 0.01
Rebalanced	0	88.64 ± 1.53	0.88 ± 0.01	0.85 ± 0.01
Rebalanced	80	86.30 ± 1.30	0.84 ± 0.02	0.83 ± 0.02

Table 2: Test set performance of fine-tuned ViT models on the `categoria` classification task. Models were (mostly) trained with a learning rate of 3×10^{-6} , a weight decay of 1×10^{-6} , and weighted loss inversely proportional to class frequency.

Head Wgts.	Acc. (%)	Prec. Sel.	Rec. Sel.
50 / 50	71.38 / 88.16	0.72 / 0.86	0.68 / 0.85
70 / 30	71.16 / 89.26	0.72 / 0.89	0.68 / 0.88
30 / 70	70.28 / 89.40	0.69 / 0.89	0.68 / 0.87

Table 3: Test set performance of fine-tuned ViT models on both `povo` and `categoria` classification tasks. For each column, the first result is directed to the `povo` head and the second one directed to the `categoria` head. Models were trained with a learning rate of 1×10^{-5} , a weight decay of 3×10^{-6} and weighted loss inversely proportional to class frequency for each head.

Rebalancing significantly improved performance, especially in precision and recall for selected classes. In contrast, partially freezing the network reduced performance,

suggesting that ViT’s lower layers required adaptation to our dataset.

Embedding spaces also revealed meaningful structure. While `povo` lacked global organization due to excluded low-sample classes, local clusters formed for well-represented groups (Figure 1 left). In the `categoria` space, coherent groupings and smooth transitions indicated a strong semantic manifold. Even excluded classes like `etnobotânica` were placed in visually appropriate regions, highlighting the model’s generalization ability (Figure 1 right).

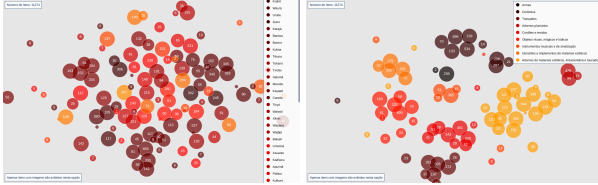


Figure 1: Embedding spaces generated by the ViT model fine-tuned on `povo` (left) and `categoria` (right). The `povo` projection shows limited global structure due to the huge amount of classes and class imbalance. The `categoria` projection displays well-defined clusters and smoother transitions, indicating a coherent underlying manifold.

Multi-head training, in turn, generally provided numeric gains, interestingly showing that joint knowledge representation enhanced learning. Single-head models, however, achieved cleaner clusters, revealing more meaningful boundaries and transitions in the embedding space.

DINOv2-Based Models: Results are summarized in Tables 4, 5 and 6.

Training Data	Frozen (%)	Acc. (%)	Prec. Sel.	Rec. Sel.
Original	0	62.73 \pm 0.62	0.53 \pm 0.02	0.65 \pm 0.01
Rebalanced	0	<u>71.46 \pm 1.13</u>	<u>0.70 \pm 0.01</u>	<u>0.67 \pm 0.01</u>
Rebalanced	80	74.70 \pm 1.24	0.74 \pm 0.03	0.71 \pm 0.01

Table 4: Test set performance of fine-tuned DINOv2 models on the `povo` classification task. Models were (mostly) trained with a learning rate of 1×10^{-6} , a weight decay of 3×10^{-7} , and weighted loss inversely proportional to class frequency.

Training Data	Frozen (%)	Acc. (%)	Prec. Sel.	Rec. Sel.
Original	0	86.60 \pm 1.44	0.84 \pm 0.03	0.83 \pm 0.02
Rebalanced	0	<u>90.21 \pm 1.22</u>	0.87 \pm 0.02	0.88 \pm 0.02
Rebalanced	80	90.52 \pm 0.64	0.87 \pm 0.01	0.88 \pm 0.01

Table 5: Test set performance of fine-tuned DINOv2 models on the `categoria` classification task. Models were (mostly) trained with a learning rate of 1×10^{-6} , a weight decay of 3×10^{-7} , and weighted loss inversely proportional to class frequency.

Even more than the previous experiments, dataset balancing significantly improved performance. In its best configurations, DINOv2 consistently outperformed ViT, achieving up to 4% higher accuracy while maintaining competitive precision and recall. Notably, this time freezing up to 80%

Head Wgts.	Acc. (%)	Prec. Sel.	Rec. Sel.
50 / 50	69.61 / 89.61	0.68 / 0.87	0.66 / 0.87
70 / 30	68.91 / 87.69	0.68 / 0.85	0.66 / 0.85
30 / 70	70.86 / 89.05	0.68 / 0.87	0.67 / 0.86

Table 6: Test set performance of fine-tuned DINOv2 models on both `povo` and `categoria` classification tasks. For each column, the first result is directed to the `povo` head and the second one directed to the `categoria` head. Models were trained with a learning rate of 3×10^{-7} , a weight decay of 1×10^{-7} and weighted loss inversely proportional to class frequency for each head.

of the model’s layers yielded performance gains, suggesting that its pretrained representations are more transferable than those of ViT. Lastly we observe that this model did not numerically benefited from the multi-head setting.

Despite the single-head quantitative improvements, DINOv2 embeddings were occasionally less interpretable when visualized in two dimensions. However, the multi-head variant preserved more semantic structure, with distinct `categoria` clusters remaining somewhat visible even under joint optimization (Figure 2).

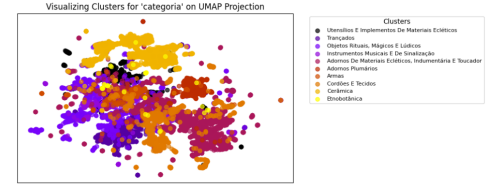


Figure 2: Embedding space of the DINOv2 multi-head model, colored by `categoria`. Despite joint supervision, `categoria` clusters remain interpretable.

Latent Observations: We highlight a few latent patterns surfaced by a ViT model fine-tuned on `categoria`. Embeddings revealed that some necklaces from the *Mayongong* community featured vibrant blue palettes, closely aligned with those of *Kamayurá* and *Kuikuro*, suggesting shared material influences (Figure 3). Outlier detection also exposed mislabeled items, such as a ceramic piece incorrectly tagged as *trançado*, yet embedded correctly among ceramics (Figure 4). These cases illustrate how semantic spaces can support curatorial analysis by uncovering hidden relationships and inconsistencies.

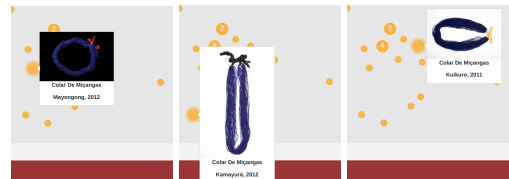


Figure 3: Visual similarities between necklaces from the *Mayongong* (left), *Kamayurá* (center), and *Kuikuro* (right) communities.

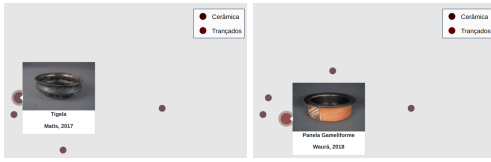


Figure 4: Typical ceramic item (left) and a misclassified outlier (right), embedded correctly by the model despite its incorrect *trançado* label.

Text-Based Semantic Spaces

Building on the image-based framework, we developed a parallel pipeline for textual data using summarized item descriptions. The goal remains consistent: to support semantic navigation and reveal latent relationships within the collection. To generate high-dimensional embeddings, we employed two sentence encoders: *BERTimbau base* (Souza, Nogueira, and Lotufo 2020), a strong starting point given its prior success in language modeling tasks, and *Albertina 100M* (Rodrigues et al. 2023), a more recent encoder with better Semantic Textual Similarity (STS) (Agirre et al. 2012) scores. We then projected embeddings into 2D using UMAP for analysis. Despite using compact versions of the models due to hardware limitations, models produced coherent and interpretable visual structures.

Fine-Tuning Strategies: To support richer exploration rather than pure classification, we shifted focus to contrastive learning on encoded sentences for directly modeling semantic similarity, particularly important for textual data, where Indigenous vocabulary challenged pre-trained models. For the unsupervised setup, we followed the unsupervised *SimCSE* framework (Gao, Yao, and Chen 2021), using a single dropout layer on top of the models and the *NT-Xent* loss (Chen et al. 2020). By running each input through the encoder twice with stochastic dropout, we obtained slightly different embeddings for the same description, which we used as a positive pair, while using other items in the batch as negative examples. This approach enabled the model to learn meaningful semantic representations without labeled data. However, due to the presence of similar descriptions in the dataset, some negative pairs were actually semantically close (false negatives), potentially reducing the effectiveness of the training signal. Despite the noise, the resulting embeddings still produced coherent local structures.

To mitigate the risk of semantically similar false negatives, we also implemented a supervised contrastive learning strategy using *InfoNCE* loss (Liao 2021) and a custom supervised contrastive learning dataset previously introduced in the data section of this paper. This setup allowed the model to explicitly align semantically related items and separate unrelated ones. While limited in scale by hardware constraints, this strategy offered a more reliable learning signal and reduced the likelihood of unintentionally penalizing similar examples.

Inspired by the work of *Liao et al.* (Liao 2021), we added a two-layer softmax classification head to the supervised

model, a configuration they showed to yield strong performance on the STS task. This not only supported more stable training but also aligned the objective of organizing the dataset around fine-grained semantic relationships.

All fine-tuned models used in our experiments were trained for 8 to 16 epochs, depending on convergence behavior and early stopping criteria. Models using the unsupervised *SimCSE* strategy converged faster, aided by the larger batch size, while the supervised *InfoNCE* models had limited batch sizes due to GPU memory constraints. We monitored training and validation loss, as well as STS-B and In-Context STS-B Pearson scores (explained in the evaluation subsection) on held-out validation subsets. Each configuration was run multiple times to report mean and standard deviation. Only the best-performing hyperparameter combinations - namely learning rate and temperature - are included in the results.

Interpretability: Unlike images, where visual differences and similarities are readily perceptible, comparing two textual descriptions is cognitively demanding. To address this, we compute attributions and highlight the specific words in each description that most influence its position in the embedding space (Figure 6).

To compute word-level attributions, we adopt the Integrated Gradients (IG) method (Sundararajan, Taly, and Yan 2017), implemented via the *Captum* library (Kokhlikyan et al. 2020). IG estimates each token’s contribution by integrating gradients along a path from a neutral baseline input to the actual description. We define our scalar output function as the cosine similarity between a given item’s final embedding and a reference point in the embedding space. This formulation allows us to attribute differences in semantic position back to specific tokens in the input, enabling more intuitive textual explanations. In practice, we discretize the integral, sum across token dimensions and compose token attributions to generate word-level scores.

Evaluation: Since our objective was not classification but semantic representation, conventional metrics like accuracy or precision and recall are no longer applicable. Instead, we assess embedding quality through STS, which quantifies how well a model’s embedding space reflects human judgments of sentence similarity. Since we are assessing models’ semantic understanding, unlike the image-based pipeline, where no baseline classifier existed, the text-based setup allows us to quantitatively compare our fine-tuned models against their vanilla counterparts and clearly demonstrate performance gains.

Differently from the image-based pipeline, in this case, since we are directly measuring the quality of semantic understanding of the models, we can compare our fine-tuned models to their vanilla counterpart and quantitatively show the performance gains.

For standardized evaluation, we rely on the Brazilian Portuguese STS-B dataset from the *extraglu* benchmark (Osório et al. 2024), a translation of the well-known *GLUE* benchmark (Wang et al. 2018). Each sentence pair in this dataset is annotated with a similarity score from 0 (unrelated) to 5 (equivalent). We compute cosine similarity be-

tween the sentence embeddings produced by our models and evaluate performance via Pearson correlation against the ground-truth scores. Although our models were not specifically fine-tuned on STS-B, they consistently outperformed their vanilla counterparts, indicating that our contrastive fine-tuning enhanced general semantic understanding. Following standard practice, due to the unavailability of labels for the official test set, we used validation set of STS-B, which we further split into validation and test subsets for our training process.

To better assess our models within domain-specific contexts, we also used a custom evaluation benchmark previously introduced in the data section: In-Context STS-B. Positive pairs were assigned a similarity score of 4 and negatives a score of 1, trying to reflect some conventions in STS-B scoring. We evaluated the models on this dataset using the same approach as before: computing cosine similarities between embeddings and measuring Pearson correlation with the assigned similarity scores. The dataset was also divided into validation and test splits. Notably, performance gains on this benchmark were often larger than on the standard STS-B, underscoring the value of this domain-adapted set as a more sensitive proxy for the kinds of semantic similarity our models aim to capture.

BERTimbau-based Models: Results are summarized in Table 7.

Learning Method	Temperature	STS-B	In-Context STS-B
Vanilla	–	0.70 ± 0.01	0.75 ± 0.01
Unsupervised	0.05	0.71 ± 0.00	0.86 ± 0.01
Unsupervised	0.2	0.74 ± 0.00	0.86 ± 0.00
Supervised	0.05	0.78 ± 0.01	0.86 ± 0.01
Supervised	0.2	0.79 ± 0.01	0.82 ± 0.00

Table 7: Parameters and test results for BERTimbau-based models. Learning rate is always set to 3×10^{-6} (when applicable).

Evaluation results highlight several trends. All fine-tuned models outperformed their vanilla counterparts, confirming the effectiveness of contrastive training. Unsupervised models showed strong improvements on the domain-specific In-Context STS-B, but smaller gains on the general STS-B, indicating specialization at the cost of generalization. Higher temperatures helped these models by softening the impact of false negatives. In contrast, supervised models achieved a better balance, with some configurations matching the unsupervised setting in domain-specific performance while substantially improving general STS-B scores. For these models, lower temperatures yielded the best average performance, likely due to the clearer learning signal from curated positives and negatives. Overall, both methods were effective, with supervised contrastive learning offering more stable and generalizable improvements.

Albertina-based Models: Results are summarized in Table 8.

As with the previous model, all fine-tuned Albertina variants outperformed the vanilla encoder on both benchmarks. However, overall performance was slightly lower compared to the BERTimbau models. While this may be

Learning Method	Temperature	STS-B	In-Context STS-B
Vanilla	–	0.69 ± 0.01	0.68 ± 0.03
Uns. SimCSE	0.05	0.70 ± 0.01	0.85 ± 0.01
Uns. SimCSE	0.1	0.72 ± 0.01	0.86 ± 0.00
InfoNCE	0.05	0.74 ± 0.01	0.87 ± 0.01
InfoNCE	0.2	0.72 ± 0.01	0.78 ± 0.01

Table 8: Parameters and test results for Albertina-based models. Learning rate is always set to 1×10^{-6} (when applicable).

surprising given that the larger Albertina variants typically outperform BERTimbau on STS benchmarks, the difference is more understandable at the base model scale. Once again, increasing the temperature in the unsupervised setup improved results, mitigating the impact of false negatives. Meanwhile, supervised models provided the most balanced performance across tasks, with lower temperature values yielding the highest scores on both general and domain-specific benchmarks.

Latent Observations: Following the quantitative evaluations, we highlight several latent patterns uncovered by a BERTimbau model fine-tuned in the supervised contrastive setting with the lowest temperature. The projected embedding space revealed well-defined local clusters, even though global structure remained limited. Zoomed-in views of the projection show tight groupings of conceptually similar items, often despite notable differences in visual appearance. For example, one cluster in the left-hand image of Figure 5 contains vases made from diverse materials and styles, grouped together through shared descriptive vocabulary that emphasizes function or theme. Another cluster, shown in the right-hand image, brings together basket-related items whose descriptions align conceptually despite lexical differences. Figure 6 illustrates two such items: while their texts use different terms like “quadrangular” and “geometrized,” both evoke geometric structure, underscoring the model’s ability to capture deep semantic relationships.



Figure 5: Zoomed-in views of UMAP projections for BERTimbau trained with supervised contrastive learning. Both regions reveal coherent and interpretable semantic clusters.

Visualization Tool

Having described the technical groundwork, we conclude with the final component of our system: an interactive visualization tool designed to make our machine learning insights accessible and explorable. Developed in Python using Plotly and Dash (Plotly Technologies Inc. 2015, 2024), the tool features three core sections: a semantic point-cloud view, a temporal acquisition timeline, and a geo-

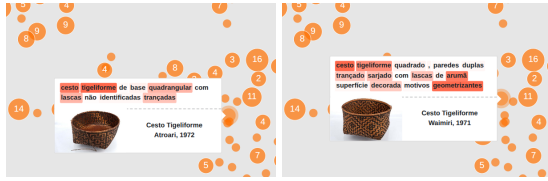


Figure 6: Two items from the basket-related cluster of the right-hand image of Figure 5 with closely aligned semantic descriptions, both placed within the same cluster.

graphic map of communities, each enabling different modes of exploration (Figure 7). Users can navigate item similarity, filter by metadata, and explore spatial or historical patterns. Built in collaboration with the *Museu Nacional dos Povos Indígenas* (mus 2025), the tool integrates feedback from multiple departments and adds features beyond the original *Tainacan* platform (tai 2025).

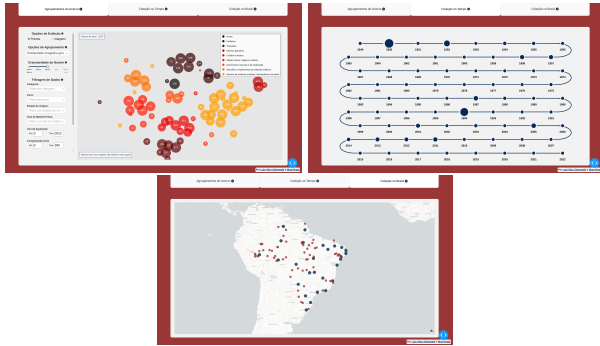


Figure 7: Primary interface tabs: collection semantic space (top-left), temporal view (top-right), geographic view (bottom).

Collection Semantic Spaces

The core of the visualization tool is the semantic point-cloud interface, where each item is displayed as a 2D point using either marker-based or image-based views. A lazy loading system ensures responsiveness by only rendering visible points, while a granularity slider controls the density of displayed items. To prevent clutter, markers collapse into clusters when zoomed out, using a viewport-sensitive KD-Tree (Bentley 1975) grouping strategy for more intuitive, screen-space aggregation. Additionally, items can be hovered (for images or summarized descriptions depending on the modality) or clicked to open full records on the *Tainacan* platform.

Multiple semantic grouping modes allow exploration through different lenses. These include the previously introduced material composition, image-based visual similarity, and textual similarity. Each mode produces distinct clustering patterns suited to different exploration goals, whether conceptual, visual, or descriptive.

A flexible filtering panel enables users to refine the dataset by multiple attributes. Filters support both multiclass values and numeric ranges. A live count keeps track of the amount of remaining items after filtering. This combination of interactive controls and semantically rich embeddings makes the

tool effective for both exploratory browsing and curatorial analysis.

Temporal View

The second main tab of the visualization tool presents a temporal interface for exploring the museum’s acquisition history, allowing users to examine how the collection evolved over time. The view consists of two interactive components: a zig-zag timeline summarizing yearly acquisition counts and a detailed breakdown for each selected year.

The top-level zig-zag timeline displays a marker for each acquisition year, with marker size reflecting item count; hovering reveals item totals, while clicking transitions to a monthly breakdown. The detailed view shows a grid of item thumbnails color-coded by acquisition month and paired with a monthly histogram. Items lacking exact dates appear first and are grouped under a separate bar in the histogram. Rich interactions include: hovering over a thumbnail to enlarge it, highlight its month, and display metadata such as item name, date, community, collection, and donor, and hovering over a histogram bar to highlight all items from that month. Navigation is paginated for the thumbnail grid to ensure interface responsiveness and naturally the hover actions are scoped per page to also prevent rendering issues. Together, these views offer a visually engaging and analytically powerful tool for temporal exploration of the collection.

Geographic View

The third tab of the visualization tool offers a geographic view of the museum’s collection, mapping items across Brazil to highlight Indigenous cultural presence. Red markers indicate specific communities (where data allows), while blue markers aggregate items by state. Clicking a marker opens a modal with item thumbnails, metadata, and optional full descriptions. Due to incomplete geographic mappings from the *Instituto Socioambiental* (ISA) (soc 2025) to our data, only around 40% of communities could be precisely located. This spatial perspective complements the semantic and temporal views, enabling users to explore regional patterns and community representation.

Conclusion and Future Work

This project aimed to support the cultural preservation of Indigenous heritage in Brazil by enhancing the *Museu Nacional dos Povos Indígenas* digital collection (mus 2025) through modern machine learning. We developed visual and textual pipelines that generated structured, machine-learning-ready representations of the collection, made available via an open-source repository. These outputs enrich curatorial work, promote public engagement, and support Indigenous visibility in the digital space, not by replacing expertise, but by complementing it with computational tools.

Future work includes dynamic updates to the system as new items are added, expanded filtering options, and visual integration of cluster centroids for improved interpretability. More advanced features like semantic search, multimodal embeddings, immersive interfaces, and 3D reconstructions using techniques like Gaussian Splatting (Kerbl et al. 2023)

could further enhance both research and public interaction. In all cases, our aim is to support intercultural dialogue and Indigenous protagonism through respectful and meaningful technological design.

Acknowledgments

We would like to express our sincere gratitude to all those who contributed to the development of this project. We are especially grateful to the *Museu Nacional dos Povos Indígenas* and its team. In particular, Seiji for serving as our primary communication with the museum and helping the project's deployment on the federal government's website; Monique for her valuable input on improving the visual tool; and Luiza for authorizing the use of the collection's images and contributing with insightful suggestions.

We would also like to thank São Paulo Research Foundation (FAPESP) – grant #2022/15304-4 for supporting this research.

References

2025. Groq. <https://groq.com/>. Accessed: 2025-07-09.
2025. Museu do Índio. <https://www.gov.br/museudoindio/pt-br>. Accessed: 2025-07-18.
2025. Socioambiental Map of Indigenous Lands. <https://mapa.socioambiental.org/pages/?lang=pt-br>. Accessed: 2025-07-09.
2025. Tainacan – Museu do Índio Collection. <https://tainacan.museudoindio.gov.br/>. Accessed: 2025-07-18.
- Agirre, E.; Cer, D.; Diab, M.; and Gonzalez-Agirre, A. 2012. SemEval-2012 Task 6: A Pilot on Semantic Textual Similarity. In Agirre, E.; Bos, J.; Diab, M.; Manandhar, S.; Marton, Y.; and Yuret, D., eds., **SEM 2012: The First Joint Conference on Lexical and Computational Semantics – Volume 1: Proceedings of the main conference and the shared task, and Volume 2: Proceedings of the Sixth International Workshop on Semantic Evaluation (SemEval 2012)*, 385–393. Montréal, Canada: Association for Computational Linguistics.
- Alma'aitah, W. Z.; Talib, A. Z.; and Osman, M. A. 2020. Opportunities and Challenges in Enhancing Access to Metadata of Cultural Heritage Collections: A Survey. *Artificial Intelligence Review*, 53: 3621–3646.
- Amid, E.; and Warmuth, M. K. 2019. TriMap: Large-scale Dimensionality Reduction Using Triplets. *CoRR*, abs/1910.00204.
- Bentley, J. L. 1975. Multidimensional binary search trees used for associative searching. *Commun. ACM*, 18(9): 509–517.
- Carter, S.; Armstrong, Z.; Schubert, L.; Johnson, I.; and Olah, C. 2019. Activation Atlas. *Distill*, 4(3): e15. <https://distill.pub/2019/activation-atlas>.
- Center for Digital Scholarship and Curation, Washington State University. 2025. Mukurtu CMS: The free, mobile and open source platform built with Indigenous communities to manage and share digital cultural heritage. <https://mukurtu.org/>. Accessed: 2025-07-18.
- Chen, T.; Kornblith, S.; Norouzi, M.; and Hinton, G. 2020. A Simple Framework for Contrastive Learning of Visual Representations. *arXiv preprint arXiv:2002.05709*.
- Dosovitskiy, A.; Beyer, L.; Kolesnikov, A.; Weissenborn, D.; Zhai, X.; Unterthiner, T.; Dehghani, M.; Minderer, M.; Heigold, G.; Gelly, S.; Uszkoreit, J.; and Houlsby, N. 2021. An Image is Worth 16×16 Words: Transformers for Image Recognition at Scale. In *International Conference on Learning Representations*.
- Ferreira, E. F. 2011. Brazilian Indigenous Peoples and the Debate on Authenticity and Cultural Change. *INDIANA - Estudos Antropológicos sobre América Latina y el Caribe*, 28: 395–408.
- Gao, T.; Yao, X.; and Chen, D. 2021. SimCSE: Simple Contrastive Learning of Sentence Embeddings. In Moens, M.-F.; Huang, X.; Specia, L.; and Yih, S. W.-t., eds., *Proceedings of the 2021 Conference on Empirical Methods in Natural Language Processing*, 6894–6910. Online and Punta Cana, Dominican Republic: Association for Computational Linguistics.
- Guimarães, S. 2015. The Teaching of Afro-Brazilian and Indigenous Culture and History in Brazilian Basic Education in the 21st Century. *Policy Futures in Education*, 13(8).
- Hisayasu, L. M. 2019. Mediated Memory and Internet Indigenous Protagonism in Brazil. Unpublished manuscript.
- Huang, Z. 1998. Extensions to the k-Means Algorithm for Clustering Large Data Sets with Categorical Values. *Data Mining and Knowledge Discovery*, 2(3): 283–304.
- Kerbl, B.; Kopanas, G.; Leimkühler, T.; and Drettakis, G. 2023. 3D Gaussian Splatting for Real-Time Radiance Field Rendering. *ACM Transactions on Graphics*, 42(4).
- Kirillov, A.; Mintun, E.; Ravi, N.; Mao, H.; Rolland, A.; Fu, T.; and Girshick, R. 2023. Segment Anything. *arXiv:2304.02643*.
- Kokhlikyan, N.; Miglani, V.; Martin, M.; Wang, E.; Alsallakh, B.; Reynolds, J.; Melnikov, A.; Kliushkina, N.; Araya, C.; Yan, S.; and Reblitz-Richardson, O. 2020. Captum: A unified and generic model interpretability library for PyTorch. *arXiv preprint arXiv:2009.07896*.
- Liao, D. 2021. Sentence Embeddings using Supervised Contrastive Learning. *CoRR*, abs/2106.04791.
- McInnes, L.; Healy, J.; and Melville, J. 2018. UMAP: Uniform Manifold Approximation and Projection for Dimension Reduction. *arXiv preprint arXiv:1802.03426*.
- Muñoz, P.; and Tisi, J. 2020. Digital Preservation and Indigenous Knowledge: Strategies and Case Studies. *Heritage Science*, 8: 45.
- Oquab, M.; Darcet, T.; Moutakanni, T.; Vo, H.; Szafraniec, M.; Khalidov, V.; Fernandez, P.; Haziza, D.; Massa, F.; El-Nouby, A.; Assran, M.; Ballas, N.; Galuba, W.; Howes, R.; Huang, P.-Y.; Li, S.-W.; Misra, I.; Rabbat, M.; Sharma, V.; Synnaeve, G.; Xu, H.; Jegou, H.; Mairal, J.; Labatut, P.; Joulin, A.; and Bojanowski, P. 2023. DINOv2: Learning Robust Visual Features without Supervision. *arXiv:2304.07193*.

Osório, T. F.; Leite, B.; Lopes Cardoso, H.; Gomes, L.; Rodrigues, J.; Santos, R.; and Branco, A. 2024. PORTULAN ExtraGLUE Datasets and Models: Kick-starting a Benchmark for the Neural Processing of Portuguese. In *Proceedings of the 17th Workshop on Building and Using Comparable Corpora (BUCC) @ LREC-COLING 2024*, 24–34. Torino, Italy: ELRA and ICCL.

Plotly Technologies Inc. 2015. Plotly: Collaborative Data Science.

Plotly Technologies Inc. 2024. Dash: A data and analytics web app framework for Python, no JavaScript required.

Radford, A.; Kim, J. W.; Hallacy, C.; Ramesh, A.; Goh, G.; Agarwal, S.; Sastry, G.; Askell, A.; Mishkin, P.; Clark, J.; Krueger, G.; and Sutskever, I. 2021. Learning Transferable Visual Models From Natural Language Supervision. In *Proceedings of the 38th International Conference on Machine Learning (ICML)*.

Rebellato, L. 2025. Digital repatriation of cultural heritage in the Global South: A model for open access to museum collections empowering indigenous communities in the Brazilian Amazon. <https://www.digarv.se/en/participating-research-projects/digital-repatriating-av-kulturarv-fran-det-globala-syd/>. Accessed: 2025-07-18.

Rodrigues, J.; Gomes, L.; Silva, J.; Branco, A.; Santos, R.; Lopes Cardoso, H.; and Osório, T. 2023. Advancing Neural Encoding of Portuguese with Transformer Albertina PT-*. *arXiv:2305.06721*.

Ronneberger, O.; Fischer, P.; and Brox, T. 2015. U-Net: Convolutional Networks for Biomedical Image Segmentation. In *Medical Image Computing and Computer-Assisted Intervention – MICCAI 2015*, 234–241. Springer.

Smilkov, D.; Thorat, N.; Nicholson, C.; Reif, E.; Viégas, F. B.; and Wattenberg, M. 2016. Embedding Projector: Interactive Visualization and Interpretation of Embeddings. *arXiv preprint arXiv:1611.05469*.

Souza, F.; Nogueira, R.; and Lotufo, R. 2020. BERTimbau: Pretrained BERT Models for Brazilian Portuguese. In *Intelligent Systems. BRACIS 2020. Lecture Notes in Computer Science*, volume 12319 of *Lecture Notes in Computer Science*, 403–417. Springer, Cham.

Steiner, A. P.; Kolesnikov, A.; Zhai, X.; Wightman, R.; Uszkoreit, J.; and Beyer, L. 2022. How to train your ViT? Data, Augmentation, and Regularization in Vision Transformers. *Transactions on Machine Learning Research*.

Sundararajan, M.; Taly, A.; and Yan, Q. 2017. Axiomatic Attribution for Deep Networks. *arXiv preprint arXiv:1703.01365*.

Touvron, H.; Lavril, T.; Izacard, G.; Martinet, X.; Lachaux, M.-A.; Lacroix, T.; Rozière, B.; Goyal, N.; Hambro, E.; Azhar, F.; Rodriguez, A.; Joulin, A.; Grave, E.; and Lample, G. 2023. LLaMA: Open and Efficient Foundation Language Models. *arXiv:2302.13971*.

van der Maaten, L.; and Hinton, G. 2008. Visualizing Data using t-SNE. *Journal of Machine Learning Research*, 9: 2579–2605.

Wang, A.; Singh, A.; Michael, J.; Hill, F.; Levy, O.; and Bowman, S. R. 2018. GLUE: A Multi-Task Benchmark and Analysis Platform for Natural Language Understanding. *arXiv:1804.07461*.

Wilder, B. T.; O’Meara, C.; Monti, L.; and Nabhan, G. P. 2016. The Importance of Indigenous Knowledge in Curbing the Loss of Language and Biodiversity. *BioScience*, 66(6): 499–509.

Zheng, P.; Gao, D.; Fan, D.-P.; Liu, L.; Laaksonen, J.; Ouyang, W.; and Sebe, N. 2024. Bilateral Reference for High-Resolution Dichotomous Image Segmentation. *CAAI Artificial Intelligence Research*.

Reproducibility Checklist

1. General Paper Structure

- 1.1. Includes a conceptual outline and/or pseudocode description of AI methods introduced (yes/partial/no/NA) [yes](#)
- 1.2. Clearly delineates statements that are opinions, hypothesis, and speculation from objective facts and results (yes/no) [yes](#)
- 1.3. Provides well-marked pedagogical references for less-familiar readers to gain background necessary to replicate the paper (yes/no) [yes](#)

2. Theoretical Contributions

- 2.1. Does this paper make theoretical contributions? (yes/no) [no](#)

If yes, please address the following points:

- 2.2. All assumptions and restrictions are stated clearly and formally (yes/partial/no) [Type your response here](#)
- 2.3. All novel claims are stated formally (e.g., in theorem statements) (yes/partial/no) [Type your response here](#)
- 2.4. Proofs of all novel claims are included (yes/partial/no) [Type your response here](#)
- 2.5. Proof sketches or intuitions are given for complex and/or novel results (yes/partial/no) [Type your response here](#)
- 2.6. Appropriate citations to theoretical tools used are given (yes/partial/no) [Type your response here](#)
- 2.7. All theoretical claims are demonstrated empirically to hold (yes/partial/no/NA) [Type your response here](#)
- 2.8. All experimental code used to eliminate or disprove claims is included (yes/no/NA) [Type your response here](#)

3. Dataset Usage

- 3.1. Does this paper rely on one or more datasets? (yes/no) **yes**

If yes, please address the following points:

- 3.2. A motivation is given for why the experiments are conducted on the selected datasets (yes/partial/no/NA) **yes**
- 3.3. All novel datasets introduced in this paper are included in a data appendix (yes/partial/no/NA) **no**
- 3.4. All novel datasets introduced in this paper will be made publicly available upon publication of the paper with a license that allows free usage for research purposes (yes/partial/no/NA) **partial**
- 3.5. All datasets drawn from the existing literature (potentially including authors' own previously published work) are accompanied by appropriate citations (yes/no/NA) **yes**
- 3.6. All datasets drawn from the existing literature (potentially including authors' own previously published work) are publicly available (yes/partial/no/NA) **yes**
- 3.7. All datasets that are not publicly available are described in detail, with explanation why publicly available alternatives are not scientifically satisfying (yes/partial/no/NA) **yes**

4. Computational Experiments

- 4.1. Does this paper include computational experiments? (yes/no) **yes**

If yes, please address the following points:

- 4.2. This paper states the number and range of values tried per (hyper-) parameter during development of the paper, along with the criterion used for selecting the final parameter setting (yes/partial/no/NA) **yes**
- 4.3. Any code required for pre-processing data is included in the appendix (yes/partial/no) **no**
- 4.4. All source code required for conducting and analyzing the experiments is included in a code appendix (yes/partial/no) **no**
- 4.5. All source code required for conducting and analyzing the experiments will be made publicly available upon publication of the paper with a license that allows free usage for research purposes (yes/partial/no) **yes**
- 4.6. All source code implementing new methods have comments detailing the implementation, with references to the paper where each step comes from (yes/partial/no) **yes**

- 4.7. If an algorithm depends on randomness, then the method used for setting seeds is described in a way sufficient to allow replication of results (yes/partial/no/NA) **partial**

- 4.8. This paper specifies the computing infrastructure used for running experiments (hardware and software), including GPU/CPU models; amount of memory; operating system; names and versions of relevant software libraries and frameworks (yes/partial/no) **partial**

- 4.9. This paper formally describes evaluation metrics used and explains the motivation for choosing these metrics (yes/partial/no) **yes**

- 4.10. This paper states the number of algorithm runs used to compute each reported result (yes/no) **yes**

- 4.11. Analysis of experiments goes beyond single-dimensional summaries of performance (e.g., average; median) to include measures of variation, confidence, or other distributional information (yes/no) **yes**

- 4.12. The significance of any improvement or decrease in performance is judged using appropriate statistical tests (e.g., Wilcoxon signed-rank) (yes/partial/no) **no**

- 4.13. This paper lists all final (hyper-)parameters used for each model/algorithm in the paper's experiments (yes/partial/no/NA) **yes**